Hydrodynamic Interaction Effects on Tugs Operating within the Midship Region alongside Large Ships

N Jayarathne [1, 2 #], Z Leong [1], D Ranmuthugala [1]

[1] *Australian Maritime College, Specialised institute of University of Tasmania, Australia*
[2] *Department of Marine Engineering, Faculty of Engineering, General Sir John Kotelawala Defence University, Sri Lanka*
[#] bnjsv@utas.edu.au

Abstract *— This paper presents the findings of a numerical and experimental study to investigate the interaction effects induced on a tug operating within the midship region of a large ship at varying drift angles and lateral distances between the vessels. The non-dimensional interaction forces and moment coefficients determined for the tug are used to create a novel Hydrodynamic Interaction Region Plot (HIRP) to identify the variation of these coefficients with respect to the tug's drift angle and relative lateral distance to the larger ship. The results identify the drift angle range for the tug required for a safe approach towards the midship of the larger ship, ensuring the least interaction induced lateral force and yaw moment in order to minimise collision risk.*

Keywords **— ship–tug interaction, drift angles, hydrodynamic interaction region plot.**

Nomenclature

C_N	Yaw moment coefficient
C_X	Surge force coefficient
C_Y	Sway force coefficient
Fr	Froude Number, Tug; $\frac{u}{\sqrt{gL_t}}$
g	Acceleration due to gravity ($9.81 m/s^2$)
HIRP	Hydrodynamic Interaction Region Plot
L_s	Waterline length of the tanker *(m)*
L_t	Waterline length of the tug *(m)*
N	Yaw moment acting on tug *(Nm)*
u	Fluid flow velocity *(m/s)*
X	Surge force acting on tug *(N)*
Y	Sway force acting on tug *(N)*
ΔY	Non-dimensionalised transverse distance between vessels
δy	least transverse distance between hulls *(m)*
ρ	Density of water (kg/m^3)
∇_s	Volumetric displacement of the tanker (m^3)
∇_t	Volumetric displacement of the tug (m^3)

I. INTRODUCTION

The hydrodynamic interaction effects between two vessels operating in close proximity can adversely affect the safety and handling of the vessels, especially if they are significantly different in size, such as a tug assisting a large tanker. During such operations, the drift angle and lateral distance between the vessels need frequent variation for accurate course keeping (Hensen, 2003). This can result in unsteady hydrodynamic interaction effects induced on the vessels, which in turn can adversely affect their ability to maintain course and speed (Hensen, 2003). The effects of these interactions can dramatically change with vessel types, width of fairway, and drift angle between the vessels (Hensen, 2003).

The majority of the hydrodynamic interaction effects studies in the past (Fortson, 1974, Newton, 1960, Zou and Larsson, 2013, Lataire et al., 2012, Chen and Fang, 2001) were carried out on vessels that are relatively similar in size and advancing on parallel courses in close proximity. However, some researchers (Dand (1975); Geerts et al. (2011); Vantorre et al. (2002); Fonfach (2010); Simonsen et al. (2011); Hensen et al. (2013)) investigated scenarios to determine the interaction effects induced on tugs operating in close proximity to large ships. Among them, Dand (1975) did a pioneering study to identify the area alongside the ships where the tugs experienced minimum interaction effects.

Dand's (1975) study utilised experimental investigations to determine interaction sway force and yaw moment induced on a tug operating near a larger ship. The latter consisted of two different ships, resulting in length ratios of 4.72 and 4.15 between each of the ships and the tug respectively. The cases investigated within Dand's study were limited to a tug operating on parallel courses at different locations along the ship, which provided the following conclusions based on the findings:

- strong cross-flow ahead of the bow of ship produces a large side force that tends to push the tug away from the ship;
- the fore-body region of a ship is a hazardous area for a tug to operate within;
- the fullness of ship affects the interaction effects; and
- the midship region of ships provide the safest location for a free running tug to approach the ship.

Based on Dand's (1975) findings, tug operators can recognize the region along the ships where they can safely operate their tugs during ship handling. However, the extent of his study was not sufficient for them to understand the best path towards the safest region (i.e. midship) along the larger ship. Furthermore, during actual tug operations, it is difficult to maintain a parallel course near the midship area of the ship throughout the manoeuvring process. Thus, it is essential to include in the study the effects of the different drift angles between the tug and the ship to determine the safe operational envelope for the tug to approach the larger ship.

The aim of this study is to investigate the variation of the interaction effects induced on a tug at different lateral distances and drift angles when operating near the midship region of a larger ship. The study uses Computational Fluid Dynamics (CFD) models, validated and supplemented through experimental model scale measurements obtained in the Australian Maritime College (AMC) model test basin, to determine the interaction effects. The non-dimensionalised interaction effects obtained enabled the creation of a Hydrodynamic Interaction Region Plot (HIRP) in order to identify the safe operational envelopes for a tug to operate near the midship during ship handling.

II. NUMERICAL STUDY

Generic model scale hulls of a stern drive tug and an MARAD-F series tanker were utilised for the CFD simulations in this study. Length ratio between the two vessels was of 1:7.03, with Table 1 outlines the vessel particulars.

Table 1. Principal dimensions of the selected hull forms.

Main Particulars	Tanker		Tug	
	Full Scale	Model Scale	Full Scale	Model Scale
Length OA (m)	210.0	4.20	31.16	1.732
Length WL (m)	200.0	4.00	28.46	1.581
Breadth (m)	36.45	0.729	11.50	0.639
Draft (m)	12.3	0.246	3.54	0.197

Fig 1 illustrates the coordinate system used for the analysis. The origin of the global coordinate system is the tanker water-plane, centre-plane, and its bow intersects, while the origin of the local coordinate system of the tug is the intersection of tug water-plane, midship plane, and its centre-plane.

The CFD simulations were carried out using the finite volume technique based StarCCM+® package via steady-state Reynolds Averaged Navier-Stokes (RANS)-based equations. The CFD simulations consisted of the following three scenarios:

- model Scale CFD simulations replicating the experimental investigations to validate the CFD simulations;
- full-Scale CFD representation of the model scale experiments for verification studies; and
- extended domain full-scale CFD simulations to investigate the cases identified in this study.

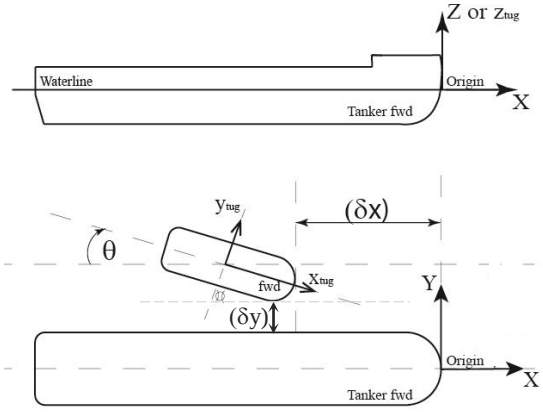

Figure 1. Global and Local (tug) coordinate systems and vessel locations.

The Model Scale CFD fluid domain replicated the captive model test conditions for validation purpose (Jayarathne et al., 2016). The validated Model Scale CFD model was then scaled by appropriate scale factors to create a full-scale

CFD simulation domain (Fig 2). The Length of the domain was 6L_S (where L_S is the tanker length) and the breadth was 1.5L_S, while the depth and the height (above the clam water free surface level) were 0.2L_S.

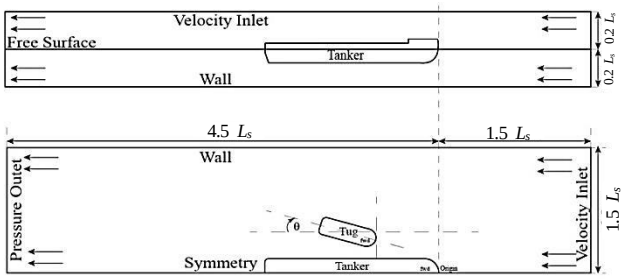

Figure 2. Computational domain.

The upstream end and the top boundaries of the domain were defined as inlets. The use of velocity inlet at the top boundary is recommended by CD-Adapco (2015) for a more robust simulation. The downstream end was maintained as a pressure outlet and the side was considered as a free-slip wall. Centre-plane through the tanker was considered as a symmetry plane to significantly reduce the mesh size similar to Fonfach (2010) study.

Both the tanker and tug geometries were locked in all degrees of freedom. As prescribed by Leong et al. (2014), a total inflation layers thickness of 1.5 times Prandtl's $1/7^{th}$ power law turbulent boundary layer thickness estimate ($1.5x0.16L_t/R_eL_t^{1/7}$) with a first near wall mesh layer distance (y^+) of 1 was used to create the mesh. The Shear Stress Transport (SST) turbulence model was used to solve the RANS equations (Fonfach, 2010).

III. EXPERIMENTAL STUDY

Captive model experiments were conducted at the Australian Maritime College's 35 m (length) x 12 m (width) x 1.0 m (depth) model test basin equipped with a multi-model carriage mechanism (Fig 3). The tanker and tug models were attached to the multi-model carriage and fixed in all degrees of freedom at the fully loaded draft, i.e. preventing any relative motion between the two models. Two strain gauges connected the tug model measured the surge and sway forces, also enabling the calculation of the yaw moment. No measurements were made of the forces and moments acting on the tanker. Details of the experimental work are given in Jayarathne et al. (2016).

Figure 3. Experimental setup for interaction between vessels in AMC's Model Test Basin.

IV. CFD VERIFICATION & VALIDATION

Numerical uncertainties were calculated according to the procedure explained by Stern et al. (2001) and Wilson et al. (2001) for the model scale and full-scale CFD models. The mesh count of the CFD models investigated in the numerical uncertainty study is outlined in Table 2.

The calculated numerical uncertainties for the finest full-scale mesh were 0.41%, 2.09% and 5.64% for the surge force, sway force and yaw moment, respectively, while they were 0.43%, 1.96% and 1.21% for the finest model scale mesh.

Table 2. Mesh resolution of the simulations used for the sensitivity study (M – Millions).

Mesh	Fine	Medium	Coarse
Model Scale	7.2M	4.8M	3.5M
Full Scale	13.2M	9.2M	6.8M

The experiment results obtained were used to validate the model scale CFD simulations. Experimental uncertainties for the forces and moments induced on the tug by the ship were calculated according to the ITTC (2002) procedure giving 7%, 9.4%, and 7%, for the surge force, sway force and yaw moment respectively (Jayarathne et al., 2016). The model scale CFD results showed good agreement with the experimental results (within 10%). Thus, when incorporating the experimental and numerical uncertainties, accuracy of the finest CFD mesh (Fig 4) was deemed acceptable for the cases investigated in this study.

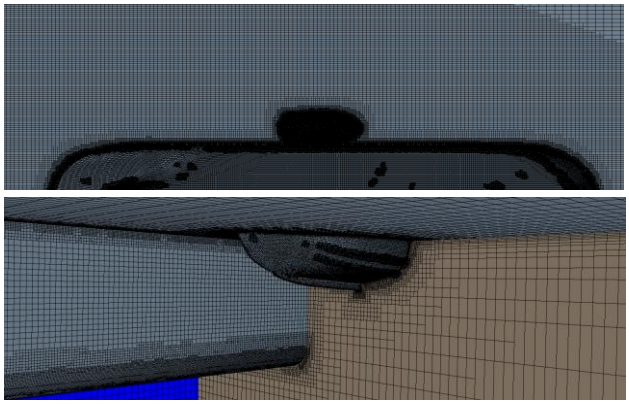

Figure 4. Selected Full-Scale Mesh – 13.2 Million Cells

Table 3. Cases investigated in the study.

Drift Angle between hulls	1 m distance between hulls Δy = 0.03	18.225 m distance between hulls Δy = 0.5	36.45m distance between hulls Δy = 1.0
0 Degree	✓	✓	✓
15 Degrees	✓	✓	✓
30 Degrees	✓	✓	✓
45 Degrees	✓	✓	✓
60 Degrees	✓	✓	✓
75 Degrees	✓	✓	✓
90 Degrees	✓	✓	✓

V. CASE STUDY

The verified and validated full scale 13.2 million CFD mesh was used to investigate the interaction effects induced on a tug operating within the midship region alongside a large tanker at three different lateral separations and seven different drift angles as given in Table 3.

Throughout the analysis, the tug was located on the port side of the tanker. Two different tug operating speeds: 3 knots (*Fr* = 0.09) and 6 knots (*Fr* = 0.18), were investigated in this study. These speeds are the minimum and maximum tug operational speeds during usual ship manoeuvring operations (Hensen, 2003). Both global and the tug local coordinate systems were used to calculate the tug's resistance against flow direction (surge force), tug's suction towards the tanker (sway force), and the moment induced on the tug due to the hydrodynamic interaction (yaw moment). Thus, the force along the x-axis of the global coordinate system was measured as the surge force (*X*), force along the y-axis of the global coordinate system was measured as the sway force (*Y*), and the moment about z-axis of the tug local coordinate system was measured as the yaw moment (*N*). The forces, moment and the lateral distance between two vessels (δy) were non-dimensionalised using Eq. 1 to Eq. 4 respectively (Fonfach, 2010, Simonsen et al., 2011).

$$C_X = \frac{2X}{u^2 \nabla_t^{1/3} \nabla_s^{1/3} \rho} \quad \text{(Eq.1)}$$

$$C_Y = \frac{2Y}{u^2 \nabla_t^{1/3} \nabla_s^{1/3} \rho} \quad \text{(Eq.2)}$$

$$C_N = \frac{2N}{u^2 \nabla_t^{1/3} \nabla_s^{1/3} L_t \rho} \quad \text{(Eq.3)}$$

$$\Delta Y = \frac{\delta y}{B_s} \quad \text{(Eq.4)}$$

V. RESULTS

A. Comparison of the Effects of Different Lateral Distances

Three different non-dimensional lateral distances were investigated in this study for drift angles ranging from zero to 90 degrees through 15 degree increments. Surge force, sway force, and yaw moment coefficients solved for each lateral distance and drift angle at the 3 knot (1.54 m/s and *Fr* = 0.09) speed are illustrated in Fig. 5.

As seen in the figure, for all lateral distances, the rate of change in surge force coefficient with respect to the drift angle was moderate between zero to 15 degree and 75 to 90 degree ranges compared to the 15 to 75 degree range. In addition, the trends look similar in all three lateral distances having a maximum surge force coefficient at the 90 degree drift angle.

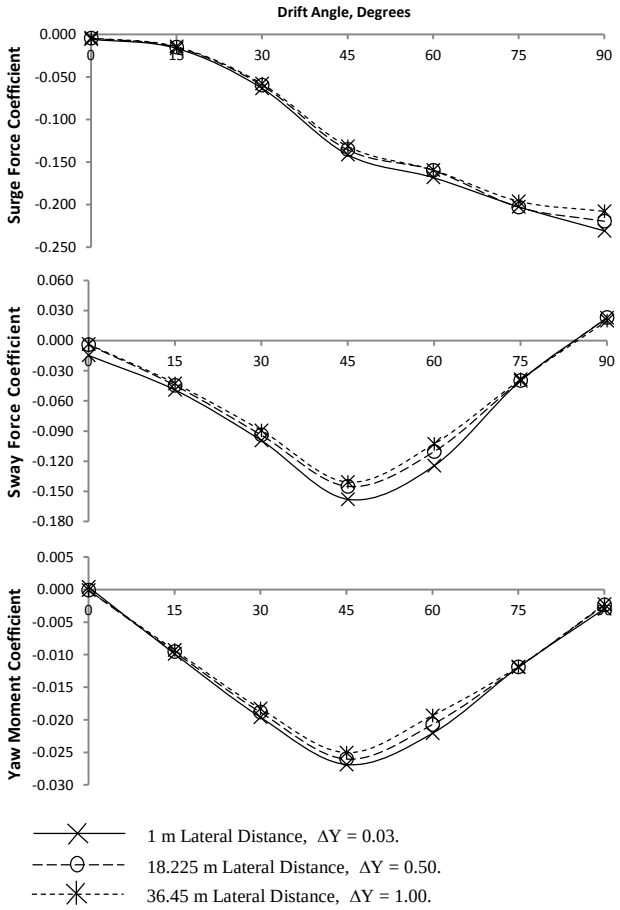

Figure 5. Surge force, sway force and yaw moment coefficients on a tug operational near a tanker at 3 knot speed with different drift angles at different non-dimensionalised lateral distances (*ΔY*).

Results trends at three lateral distances for the sway force coefficient (tug's suction towards the tanker) were significantly different from that for the surge. From zero (parallel) to 45 degrees drift angle, the sway force coefficient increases and then on decreases at a similar rate as the drift angle approaches 90 degrees. The tug experiences the maximum suction towards the tanker within the 40 to 50 degrees drift angle range. Around the 90 degree drift angle, the tug experiences a push away force (positive sway) due to tanker's hydrodynamic effects. Nevertheless, the trends for the three lateral distances showed an increase with decreasing lateral distance between the tug and the tanker, which is similar to that for the surge force coefficients, with the largest difference between the three around the 45 degree drift angle.

The yaw moment coefficient follows a similar trend to the sway force coefficient, except for 90 degrees. From zero to 45 degrees drift angle the yaw moment increases to a maximum and then decreases as the drift angle increases to 90 degrees. Maximum yaw moment coefficient is around a drift angle around 40 to 50 degrees. Similar to the surge and sway force coefficients, the yaw moment coefficient also increases with decreasing lateral distances in a similar trend.

Among the three interaction effects considered, the sway force and the yaw moment are the most significant affecting the safety of the tug (Dand, 1975, Hensen, 2003). Due to its unpredictable nature, tug masters need sufficient knowledge and experience to understand whether their tug would be pulled, pushed, or turned by the larger ships' flow hydrodynamics (Hensen, 2003). Considering the sway force and yaw moment, it is seen that except for small (zero to 15 degrees) or large (75 to 90 degrees) drift angles, the latter can have a critical influence on the safety of a tug to operating in close proximity to a larger vessel like a tanker in its midship region. Thus, for a tug, if it is not possible to follow a parallel course to approach the midship region of the larger vessel, it is safer to select a path within zero to 15 degrees or 75 to 90 degrees drift angle ranges to minimise the collision risk.

Although the results for the 6 knot (3.09 m/s and *Fr* = 0.18) speed are not discussed here, they display similar trends, with the calculated surge force, sway force and yaw moment coefficients lying within 9.5% of the results for 3 knots shown in Figure 5.

B. Comparison of Pressure Plots

The pressure plots around the vessels for 6 knots (*Fr* = 0.18*)* and a non-dimensionalised lateral distance (*ΔY*) of 0.03 are presented in Figure 6. This enables the pressure variation to be considered in identifying a safe operational envelope for a tug operating in close proximity to the midship region of the larger ship.

As seen in Figure 6, as the drift angle increases, the pressure on the starboard side of the tug (i.e. leeward side) decreases significantly. At large drift angles (> 45 degrees), the pressure difference between the bow and stern regions of the tug are not significant due to the large extended low-pressure region totally encompassing its starboard side. Thus, the yaw moment induced on tug reduces as the drift angle increased beyond 45 degrees.

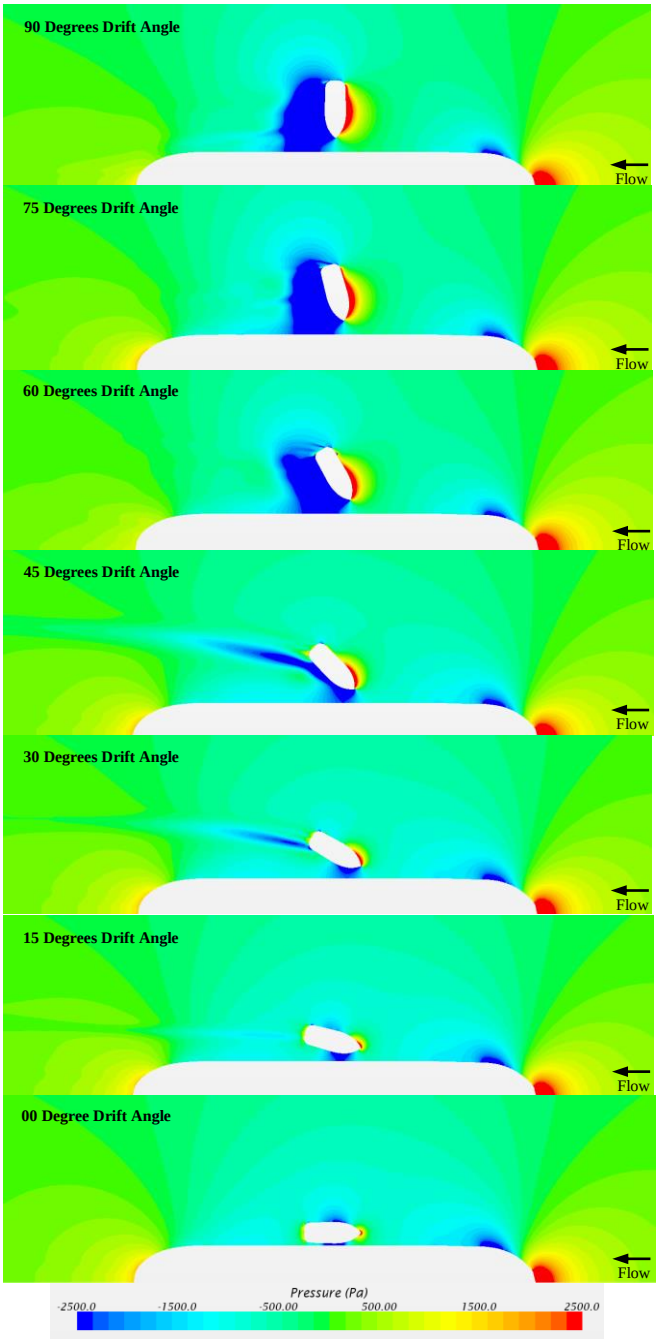

Figure 6. Pressure plots around the vessels at 6 knots (*Fr* = 0.18) speed with different drift angle from zero to 90 degrees at the non-dimensionalised lateral distance, ΔY, of 0.03.

Furthermore, from zero to 45 degrees, the low-pressure region between two ships shows a noteworthy increment, with the maximum suction towards the tanker occurring around 45 degrees. However, as the drift angle increases beyond 45 degrees, the parallel length between two ships decreases. Therefore, it caused a notable reduction in the low-pressure affected area on the tug adjacent to the ship; thus reducing the suction of the tug towards it (i.e. reducing the sway force).

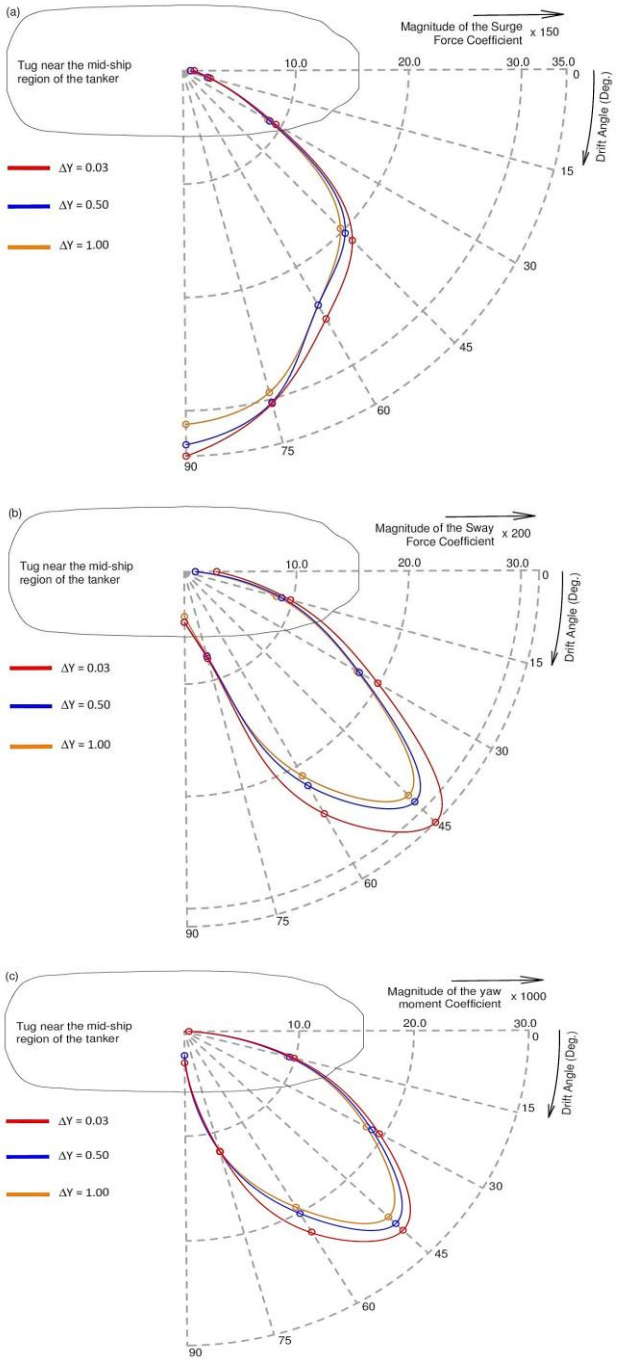

Figure 7. Hydrodynamic Interaction Region Plots (HIRP) to identify the safe paths for a tug to approach the midship region of a larger vessel.

a) Magnitude of the surge force coefficient;
b) Magnitude of the sway force coefficient;
c) Magnitude of the yaw moment coefficient.

Considering the surge force acting on the tug along the global x-axis, since both the pressure difference and the projected area it affects (increasing to that of the full length of the tug at 90 degrees) increases as the drift angle increases, the corresponding surge force increases significantly with the drift angle (see Figure 5 for the trend). When the vessels are in parallel, due to the relatively streamlined hull the pressure difference is relatively low, although tugs with large transoms may experience higher values. In addition, the projected area is at the lowest at this angle.

VI. HYDRODYNAMIC INTERACTION REGION PLOT (HIRP)

In order to identify the safe locus for a tug to approach the midship region of a large ship, the overall findings of this study are presented as "Hydrodynamic Interaction Region Plots" (HIRP) as shown in Figure 7. As it was shown earlier in the discussions that the sway force and yaw moment were the critical factors that affected the safety of the tug, their magnitudes were selected as the parameters for the HIRP representation. According to HIRP, the drift angle ranges between zero to 15 degrees and 75 to 90 degrees are the safest, with minimum sway force and yaw moment induced on the tug. Although it is safe within the 75 to 90 degree range, the tug master should be aware that the tug would experience maximum resistance due to the incoming flow within this drift angle range.

At the drift angle range between 40 to 50 degrees, the tug will experience the maximum interaction effects. Thus, it is advisable to avoid such angles during ship manoeuvring operations, thus requiring the tug master to move quickly through that range when increasing or decreasing the tug's drift angle relative to the larger vessel. Drift angle ranges between 15 to 40 degrees, and 50 to 75 degrees, has incrementing and decrementing interaction effects respectively, where the tug master should be cautious of the change in interaction behaviour in order to avoid under or overcompensating it during related manoeuvres.

V. CONCLUSION

The aim of this study was to investigate the variation of the interaction effects induced on a tug with different lateral distances and drift angles when operating in close proximity to the midship region of a larger ship. Verified and validated CFD simulations together with model scale experimental results were used to determine the interaction effects for a number of drift angles, lateral distances, and speeds. The results were presented on a novel region plots, titled the Hydrodynamic Interaction Region Plots (HIRP), enabling the tug operators to identify the safest operational envelopes for a tug to approach the midship region of the larger ship.

The results revealed that drift angles ranging from zero to 15 degrees and 75 to 90 degree present least interaction sway force and yaw moment. Thus, when a tug is approaching the midship region of the larger vessel, it has to follow a path within the above safe ranges ensuring the least suction and yaw moment to minimise the risk of collision. Once the tug reaches the midship region of the larger vessel, it is safer to follow a parallel course with the latter.

The study also identified drift angles between 40 to 50 degrees as the critical, and should be avoided to reduce the risk of collision between vessels. It was also noted that at large drift angles, the surge forces are relatively high, which may cause difficulty in maintaining position relative to the larger vessel. In the angles between the critical and safe ranges, the relevant forces and moment changed rapidly as the drift angle changed. Thus, it is advisable to maintain the drift angles only within the safe ranges, moving quickly through the adverse ranges.

The results of this study will be further extended in future studies to develop a comprehensive HIRP for tug masters to understand safe operational envelopes for close proximity operations with a larger ship at any location.

ACKNOWLEDGMENT

Authors would like to acknowledge the extensive support given by AMC Model Test Basin staff during the experiments.

REFERENCES

Cd-Adapco (2015). User Manual of StarCCM+ Version 10.02.

Chen, G. R. & Fang, M. C. (2001). Hydrodynamic Interactions Between Two Ships Advancing in Waves. *Ocean Engineering,* 28**,** 1053-1078.

Dand, I. W. (1976). Some Aspects of Tug-Ship Interaction. *In:*Troup, K. D., ed. The Fourth International Tug Convention, 1975 New Orleans, Louisiana, USA. Thomas Reed Industrial Press LTD, 300.

Fonfach, J. M. A. (2010). *Numerical Study of the Hydrodynamic Interaction Between Ships in Viscous and Inviscid Flow.* Instituto Superior Tecnico.

Fortson, R. M. (1974). *Interaction Force Between Ships.* Ocean Engineering, Massachusetts Institute of Technology.

Geerts, S., Vantorre, M., Eloot, K., et al. (2011). Interaction Forces in Tug Operation. *In:*Pettersen, B., Berg, T. E., Eloot, K., et al., eds. 2nd International Conference on Ship Manoeuvring in Shallow and Confined Water: Ship to Ship Interaction, 2011 Trondheim, Norway. The Royal Institute of Naval Architects, 441.

Hensen, H. (2003). *Tug Use in Port: A Practical Guide*, Nautical Institute.

Hensen, H., Merkelbach, D. & Wijnen, F. V. (2013). Report on Safe Tug Procedures. Netherlands: Dutch Safety Board.

ITTC (2002). Testing and Extrapolation Methods - Resistance Uncertainty Analysis. International Towing Tank Conference.

Jayarathne, B. N., Ranmuthugala, D., Leong, Z. Q., et al. (2016). Numerical Prediction of Ship-Tug Interaction Effects. *Journal of Ship Research*.[Under-Review]

Lataire, E., Vantorre, M., Delefortrie, G., et al. (2012). Mathematical Modelling of Forces Acting on Ships During Lightering Operations. *Ocean Engineering,* 55**,** 101-115.

Leong, Z. Q., Ranmuthugala, D., Penesis, I., et al. (2014). RANS-Based CFD Prediction of the Hydrodynamic Coefficients of DARPA SUBOFF Geometry in Straight-Line and Rotating Arm Manoeuvres. *Transactions RINA: Part A1-International Journal Maritime Engineering*.

Newton, R. N. (1960). Some Notes on Interaction Effects Between Ships Close Aboard in Deep Water. First Symposium on Ship Maneuverability, 1960 Washington D. C.: U.S. Government Printing Office, 423.

Simonsen, C. D., Nielsen, C. K., Otzen, J. F., et al. (2011). CFD Based Prediction of Ship-Ship Interaction Forces on a Tug Beside a Tanker. *In:*Pettersen, B., Berg, T. E., Eloot, K., et al., eds. 2nd International Conference on Ship Manoeuvring in Shallow and Confined Water: Ship to Ship Interaction, 2011 Trondheim, Norway. The Royal Institute of Naval Architects, 441.

Stern, F., Wilson, R. V., Coleman, H. W., et al. (2001). Comprehensive Approach to Verification and Validation of CFD Simulations - Part 1: Methodology and Procedures. *Journal of Fluids Engineering,* 123**,** 793-802.

Vantorre, M., Verzhbitskaya, E. & Laforce, E. (2002). Model Test Based Formulations of Ship-Ship Interaction Forces. *Ship Technology Research,* 49**,** 124-141.

Wilson, R. V., Stern, F., Coleman, H. W., et al. (2001). Comprehensive Approach to Verification and Validation of CFD Simulations - Part 2: Application for RANS Simulation of a Cargo/Container Ship. *Journal of Fluids Engineering,* 123**,** 803-810.

Zou, L. & Larsson, L. (2013). Numerical Predictions of Ship-to-Ship Interaction in Shallow Water. *Ocean Engineering,* 72**,** 386–402.